Analytical models of lateral power devices with arbitrary vertical doping profiles in the drift region*

Hua Ting-Ting(花婷婷)[a], Guo Yu-Feng(郭宇锋)[a]†, Yu Ying(于 映)[a], Gene Sheu[b], Jian Tong(蹇 彤)[a], and Yao Jia-Fei(姚佳飞)[a]

[a] College of Electronic Science and Engineering, Nanjing University of Posts and Telecommunications, Nanjing 210003, China
[b] Department of Computer Science & Information Engineering, Asia University, Taiwan 41354, China

(Received 10 October 2012; revised manuscript received 10 December 2012)

By solving the 2D Poisson's equation, analytical models are proposed to calculate the surface potential and electric field distributions of lateral power devices with arbitrary vertical doping profiles. The vertical and the lateral breakdown voltages are formulized to quantify the breakdown characteristic in completely-depleted and partially-depleted cases. A new reduced surface field (RESURF) criterion which can be used in various drift doping profiles is further derived for obtaining the optimal trade-off between the breakdown voltage and the on-resistance. Based on these models and the numerical simulation, the electric field modulation mechanism and the breakdown characteristics of lateral power devices are investigated in detail for the uniform, linear, Gaussian, and some discrete doping profiles along the vertical direction in the drift region. Then, the mentioned vertical doping profiles of these devices with the same geometric parameters are optimized, and the results show that the optimal breakdown voltages and the effective drift doping concentrations of these devices are identical, which are equal to those of the uniform-doped device, respectively. The analytical results of these proposed models are in good agreement with the numerical results and the previous experimental results, confirming the validity of the models presented here.

Keywords: surface electric field, breakdown voltage, optimization

PACS: 85.30.De, 85.30.Tv, 84.70.+p **DOI:** 10.1088/1674-1056/22/5/058501

1. Introduction

The reduced surface field (RESURF) technology has been widely used in lateral power devices. It can lower the on-resistance and reduce the chip size of a lateral power device while maintaining a high breakdown voltage.[1–3] The electric field distribution in the drift region of a device is of great significance, especially due to the involved RESURF effect. In recent years, several analytical models of RESURF devices have been introduced.[4–10] Based on solving 2D Poisson's equation, Chung *et al.* obtained the analytical models of surface potential and electric field distributions for the first time.[5] He *et al.* obtained the expressions of surface potential and electric field distributions by utilizing the integral form of the 2D Poisson's equation, and further discussed the optimization of the breakdown voltage.[6] Li *et al.* presented a full breakdown model for both the completely-depleted and partially-depleted cases.[7] However, those models are all for epitaxial RESURF devices in which the drift doping profiles are considered to be uniform. In fact, the uniform-doped drift region cannot be satisfied in many cases. For example, to be suited for advanced technology processing, the drift region is formed by a lightly-doped N-well region, so the vertical doping profile is Gaussian.[10–12] References [13]– [16] presented a buried P-type layer structure in which the vertical doping profile is discrete, realizing a good trade-off between the breakdown voltage and the on-resistance. In addition, some researchers believed that the vertical linear doping lateral double-diffused metal-oxide-semiconductor (LDMOS) exhibits a superior performance.[17,18] Obviously, the vertical doping profile in the drift region can be various. To the best of our knowledge, there has not been any general analytical model of a lateral power device so far which is suitable for arbitrary drift vertical doping profile.

The purpose of this paper is to present analytical models for bulk silicon RESURF devices with arbitrary vertical doping profile. Based on the 2D Poisson's equation, the solutions of surface potential and electric field distributions for completely-depleted and partially-depleted RESURF devices are derived. Then, the breakdown voltage due to the electric field peak is calculated. In addition, the quantified optimum criterion for the maximum breakdown voltage and a lower on-resistance is obtained. According to the proposed model and numerical simulation, surface electric field distributions and breakdown voltages of RESURF LDMOS devices with different vertical doping profiles are investigated. The optimal vertical doping profiles and the overall electrical performances of

*Projects supported by the National Natural Science Foundation of China (Grant No. 61076073), the Natural Science Foundation of Jiangsu Higher Education Institutions of China (Grant No. 09KJB510010), the Open Foundation of State Key Laboratory of Electronic Thin Films and Integrated Devices, China (Grant No. KFJJ201011), and the Research and Innovation Project for College Graduates of Jiangsu Province, China (Grant No. CXZZ11_0382).

†Corresponding author. E-mail: yfguo@njupt.edu.cn

© 2013 Chinese Physical Society and IOP Publishing Ltd

these devices are also examined.

2. Surface potential/electric-field model

A schematic cross-section of a RESURF LDMOS device with arbitrary drift vertical doping profile is shown in Fig. 1(a), where x measures the horizontal position relative to the left edge of the drift region, y measures the vertical position relative to the surface of the drift region, and t_s is the epitaxial silicon thickness with permittivity ε_s. The drift region length is L_d; $N(y)$ represents the doping concentration of the drift region, where $0 \le y \le t_s$. The substrate doping concentration is N_A. The drain of the device is biased to a positive voltage V_d, while the source, the gate, and the substrate are grounded. The lateral depletion width and the vertical depletion thickness are denoted as W_d and t_v, respectively; and t_b is the depletion thickness within the substrate.

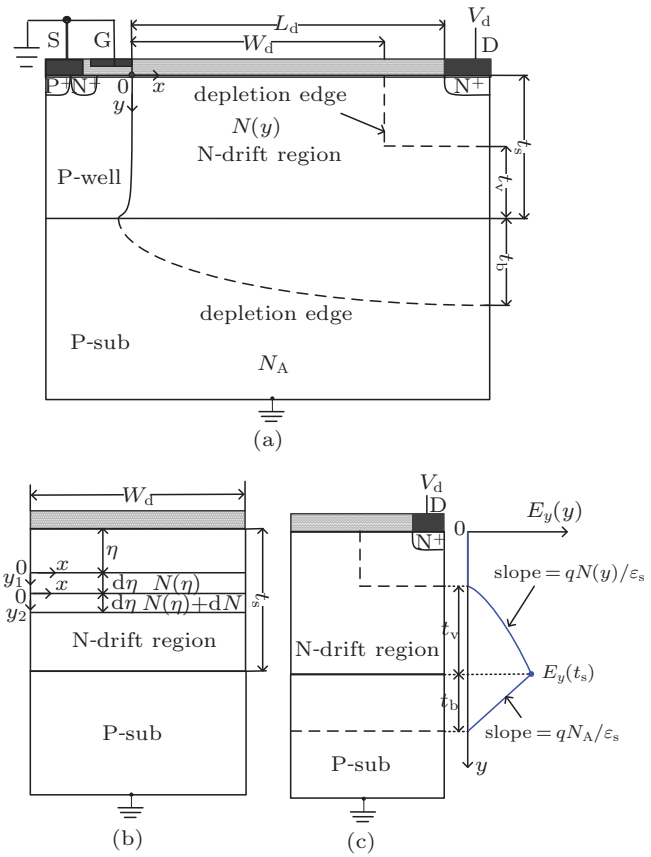


Fig. 1. RESURF LDMOS device with arbitrary vertical doping profile. (a) Schematic cross-section of the proposed device structure, (b) coordinates and variables for the depletion, (c) vertical electric field distribution under the drain.

In the depletion, we take two neighborhood layers arbitrarily at $y = \eta$ with thickness $d\eta$ as shown in Fig. 1(b). When $d\eta$ is small enough, the two layers can be regard as uniformly-doped, and the impurity concentrations are denoted as $N(\eta)$ and $N(\eta) + dN$, respectively. The potential functions in the two layers obey the 2D Poisson's equation

$$\frac{\partial^2 \varphi_1(x,y_1)}{\partial x^2} + \frac{\partial^2 \varphi_1(x,y_1)}{\partial y_1^2} = -\frac{qN(\eta)}{\varepsilon_s}, \quad (0 \le x \le W_d, \quad 0 \le y_1 \le d\eta),$$
$$\frac{\partial^2 \varphi_2(x,y_2)}{\partial x^2} + \frac{\partial^2 \varphi_2(x,y_2)}{\partial y_2^2} = -\frac{q[N(\eta)+dN]}{\varepsilon_s}, \quad (0 \le x \le W_d, \quad 0 \le y_2 \le d\eta). \tag{1}$$

The electrostatic potentials of the two neighborhood layers can be approximated[19] by simple parabolic functions

$$\begin{aligned} \varphi_1(x,y_1) &= a(\eta) + b(\eta)y_1 + c(\eta)y_1^2, \\ \varphi_2(x,y_2) &= [a(\eta)+da] + [b(\eta)+db]y_2 \\ &\quad + [c(\eta)+dc]y_2^2, \end{aligned} \tag{2}$$

where coefficients $a(\eta)$, $b(\eta)$, and $c(\eta)$ are only functions of x when $y = \eta$ is given.

Using the continuities of the potential, the electric field, and the doping along the interface of the two layers, the potential functions satisfy

$$\varphi_1(x, d\eta) = \varphi_2(x, 0), \tag{3}$$
$$\left.\frac{\partial \varphi_1(x,y_1)}{\partial y_1}\right|_{y_1 = d\eta} = \left.\frac{\partial \varphi_2(x,y_2)}{\partial y_2}\right|_{y_2=0}, \tag{4}$$
$$\frac{\partial^2 \varphi_1(x, d\eta)}{\partial x^2} = \frac{\partial^2 \varphi_2(x,0)}{\partial x^2}. \tag{5}$$

Substituting Eq. (2) into the continuity conditions (3)–(5), we obtain the differential equations

$$\begin{cases} \dfrac{d^2 a}{d\eta^2} = \dfrac{b(\eta)}{d\eta} + c(\eta), \\ \dfrac{db}{d\eta} = 2c(\eta), \\ \dfrac{dc}{d\eta} = -\dfrac{q}{2\varepsilon_s}\dfrac{dN}{d\eta}. \end{cases} \tag{6}$$

Then by calculating the integral in Eq. (6) along the path of 0–y, the following expressions are derived:

$$\begin{cases} a(y) = a(0) + c(0)y^2 - \dfrac{q}{2\varepsilon_s}\displaystyle\int_0^y dN \left(\int_\eta^y d\eta\right)^2, \\ b(y) = b(0) + 2c(0)y - \dfrac{q}{\varepsilon_s}\displaystyle\int_0^y dN \int_\eta^y d\eta, \\ c(y) = c(0) - \dfrac{q}{2\varepsilon_s}[N(y) - N(0)]. \end{cases} \tag{7}$$

Taking into account the continuity of electric flux density across the top and the bottom boundaries of the epitaxial silicon,[8] we obtain

$$b(0) = 0, \quad b(t_s) = -\frac{2a(t_s)}{t_b}. \tag{8}$$

With the substitution of Eq. (7) into Eq. (8), the following relation between $a(0)$ and $c(0)$ can be obtained:

$$c(0) = -\frac{1}{2t^2}\left\{a(0) - \frac{q}{\varepsilon_s}[N_{\text{eff}} - N(0)]t^2\right\}, \tag{9}$$

where t is defined as the characteristic thickness and is written as

$$t = \sqrt{\frac{t_b}{2}t_s + \frac{t_s^2}{2}}, \tag{10}$$

and $N_{\rm eff}$ denotes the effective concentration and is expressed as

$$N_{\rm eff} = \frac{1}{t^2}\int_0^{t_s} N(\eta)\left(t_s + \frac{t_b}{2} - \eta\right) {\rm d}\eta. \tag{11}$$

Combining Eq. (9) and the 2D Poisson's equation leads to a differential equation for the surface potential distribution function $\varphi(x,0)$

$$\frac{\partial^2 \varphi(x,0)}{\partial x^2} - \frac{\varphi(x,0)}{t^2} = -\frac{qN_{\rm eff}}{\varepsilon_s}. \tag{12}$$

Solving Eq. (12) with the boundary values of $\varphi(0,0) = 0$ and $\varphi(W_d,0) = V_d$ yields

$$\begin{aligned}\varphi(x,0) &= V_0 + (V_d - V_0)\frac{\sinh(x/t)}{\sinh(W_d/t)} \\ &\quad - V_0\frac{\sinh[(W_d - x)/t]}{\sinh(W_d/t)},\end{aligned} \tag{13}$$

where $V_0 = qN_{\rm eff}t^2/\varepsilon_s$. By differentiating Eq. (13), the surface electric field distribution is obtained as

$$E_x(x,0) = (V_d - V_0)\frac{\cosh(x/t)}{t\sinh(W_d/t)} + V_0\frac{\cosh[(W_d - x)/t]}{t\sinh(W_d/t)}. \tag{14}$$

The lateral depletion width W_d in Eqs. (13) and (14) satisfies

$$W_d = \begin{cases} t\,{\rm arccosh}\left(\dfrac{V_0}{V_0 - V_d}\right), & V_d < V_0\left[1 - {\rm sech}(L_d/t)\right], \\ L_d, & V_d \geq V_0\left[1 - {\rm sech}(L_d/t)\right]. \end{cases} \tag{15}$$

When $V_d < V_0[1 - {\rm sech}(L_d/t)]$, the drift region is partially-depleted, W_d can be obtained by substituting Eq. (14) into $E_x(W_d,0) = 0$. For the case with $V_d \geq V_0[1 - {\rm sech}(L_d/t)]$, the whole boxed drift region is completely-depleted, W_d equals L_d.

In the vertical direction, we neglect the influence of the drain junction depth and assume a uniform substrate depletion thickness t_b at the first-order approximation.[6] Then, based on the basic theory of the double-sided PN junction, the vertical electric field distribution along the drain edge is approximately obtained as shown in Fig. 1(c).[20] The applied drain voltage V_d is thus given by

$$V_d = \frac{1}{2}\frac{qN_A}{\varepsilon_s}(t_b)^2 + \int_{t_s - t_v}^{t_s}\int_{t_s - t_v}^{y}\frac{qN(\eta)}{\varepsilon_s}{\rm d}\eta\,{\rm d}y. \tag{16}$$

The vertical electric field peak is expressed as

$$E_y(t_s) = \frac{qN_A}{\varepsilon_s}t_b = \int_{t_s - t_v}^{t_s}\frac{qN(\eta)}{\varepsilon_s}{\rm d}\eta. \tag{17}$$

Combining Eq. (16) with Eq. (17), we obtain a quadratic equation

$$t_b = t_v\left(\sqrt{1 + 2\frac{\varepsilon_s(V_d + V_f)}{qN_A t_v^2}} - 1\right), \tag{18}$$

where

$$V_f = \int_{t_s - t_v}^{t_s}\int_{y}^{t_s}\frac{qN(\eta)}{\varepsilon_s}{\rm d}\eta\,{\rm d}y$$

has the voltage unit and relies on the vertical doping profile of the drift region, t_v is equal to the epitaxial silicon thickness t_s when the drift region is completely-depleted. Otherwise, by substituting Eq. (18) into Eq. (17) and utilizing the software Matlab, t_v and thus t_b can be solved.

3. Breakdown voltage model

For RESURF devices, the avalanche breakdown occurs at the location with the maximum electric field. A useful parameter to identify the onset of avalanche breakdown within the device is the critical electric field;[21] when the maximum electric field in the device exceeds the critical electric field, the device breaks down. For the case that the drift region is completely-depleted, the electric field peaks are at the surfaces of the P-well/N-drift and N-drift/N^+-drain junctions and at the interface of drift/substrate under the drain. Substituting Eq. (14) into the breakdown condition $[E_x(0,0), E_x(L_d,0)] = E_{c,\rm lat}$ yields the lateral breakdown voltage

$$V_{B,cd}^{PN} = E_{c,\rm lat}t\sinh(L_d/t) + V_0[1 - \cosh(L_d/t)], \tag{19}$$

$$V_{B,cd}^{NN} = E_{c,\rm lat}t\tanh(L_d/t) + V_0[1 - {\rm sech}(L_d/t)], \tag{20}$$

where $V_{B,cd}^{PN}$ and $V_{B,cd}^{NN}$ are the breakdown voltages when the breakdown occurs at the surfaces of the P-well/N-drift and N-drift/N^+-drain junctions, respectively, and $E_{c,\rm lat}$ denotes the critical electric field when the breakdown occurs in the lateral direction. By substituting Eq. (17) of the vertical electric field peak into the breakdown condition $E_y(t_s) = E_{c,\rm ver}$, where $E_{c,\rm ver}$ denotes the critical electric field when the breakdown occurs in the vertical direction, the vertical breakdown voltage $V_{B,cd}^{\rm ver}$ is obtained as

$$V_{B,cd}^{\rm ver} = \frac{\varepsilon_s E_{c,\rm ver}^2}{2qN_A} + E_{c,\rm ver}t_s - V_f. \tag{21}$$

For a low applied voltage, the drift region is partially-depleted and $E_x(W_d,0) = 0$. In this case, the electric field peaks are at the surface of the P-well/N-drift junction and at the interface of drift/substrate under the drain. The breakdown voltage can be obtained from $E_x(0,0) = E_{c,\rm lat}$ and $E_y(t_s) = E_{c,\rm ver}$, so the lateral breakdown voltage $V_{B,pd}^{PN}$ and the vertical breakdown voltage $V_{B,pd}^{\rm ver}$ are expressed as

$$V_{B,pd}^{PN} = E_{c,\rm lat}t\sinh(W_d/t) + V_0[1 - \cosh(W_d/t)], \tag{22}$$

$$V_{\mathrm{B,pd}}^{\mathrm{ver}} = \frac{\varepsilon_{\mathrm{s}} E_{\mathrm{c,ver}}^2}{2qN_{\mathrm{A}}} + E_{\mathrm{c,ver}} t_{\mathrm{v}} - V_{\mathrm{f}}. \tag{23}$$

In fact, there is only one position at which the breakdown occurs. So the breakdown voltage of the completely-depleted case is $V_{\mathrm{B,cd}} = \mathrm{Min}\left[V_{\mathrm{B,cd}}^{\mathrm{PN}}, V_{\mathrm{B,cd}}^{\mathrm{NN}}, V_{\mathrm{B,cd}}^{\mathrm{ver}}\right]$ and the breakdown voltage of the partially-depleted case is $V_{\mathrm{B,pd}} = \mathrm{Min}\left[V_{\mathrm{B,pd}}^{\mathrm{PN}}, V_{\mathrm{B,pd}}^{\mathrm{ver}}\right]$.

4. RESURF criterion

The main objective in optimizing the RESURF LDMOS device is to minimize the on-resistance and maximize the breakdown voltage. This can be achieved if the drift region is designed such that it is completely-depleted and the two surface electric field peaks at the drift region edges are equal to each other when the breakdown occurs.[6] By substituting Eq. (14) into $E_x(0,0) = E_x(L_{\mathrm{d}},0)$, the optimal lateral breakdown voltage is derived as follows:

$$V_{\mathrm{B,lat.opt}} = 2qN_{\mathrm{eff}}t^2/\varepsilon_{\mathrm{s}}. \tag{24}$$

To ensure that the breakdown occurs due to the high electric field at the drift/substrate junction rather than at the surface, the optimum criterion of $V_{\mathrm{B,lat.opt}} \geq V_{\mathrm{B,cd}}^{\mathrm{ver}}$, $E_x(0,0) = E_x(L_{\mathrm{d}},0) \leq E_{\mathrm{c.lat}}$ should be satisfied. As a result,

$$\frac{\varepsilon_{\mathrm{s}} E_{\mathrm{c,ver}}}{2q} \leq N_{\mathrm{eff}}t \leq \frac{\varepsilon_{\mathrm{s}} E_{\mathrm{c,lat}}}{q}. \tag{25}$$

This is a generalized RESURF criterion for lateral power devices with arbitrary vertical doping profiles in the drift region. For the uniform drift doping, it reduces to the format illustrated in Ref. [6]. By utilizing Eqs. (24) and (25), we can determine the optimal drift doping profile when the geometric parameters of the device and an anticipated breakdown voltage are given.

5. Results and discussion

In order to verify the proposed analytical models, the lateral power devices with different vertical doping profiles are numerically simulated using 2D semiconductor device simulating tools, Medici. Table 1 gives the analytical expressions of different vertical doping profiles. To assist our analysis, figure 2 shows the schematic cross-sections of RESURF LDMOS devices with the discussed discrete doping profiles. For continuous doping profiles, the surface potential and electric field distributions can be obtained just by substituting the analytical expressions of the vertical doping profiles into Eqs. (13) and (14). While for discrete doping profiles, due to the complexity of the depletion edge in the partially-depleted case, our proposed models are only suitable for the completely-depleted case. During the calculation, we first divide the whole drift region into several regions according to the vertical doping profile, then use the proposed analytical models separately in each region, and finally utilize the continuity conditions of the lateral electric fields to obtain the surface potential and electric field distributions.[14]

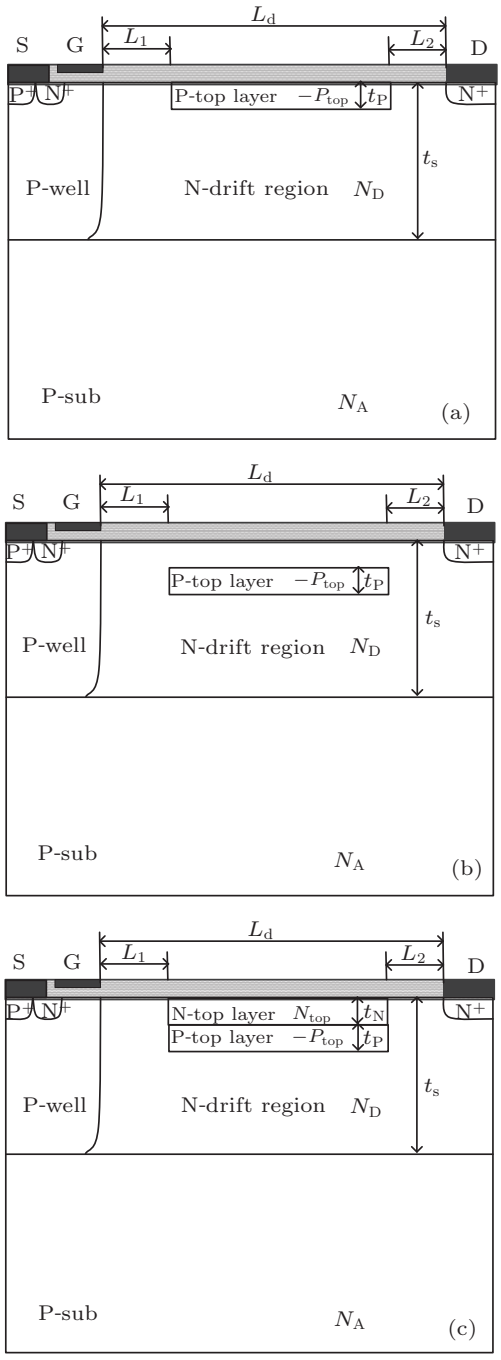


Fig. 2. Schematic cross-sections of RESURF LDMOS devices with discrete vertical doping profiles: (a) D-RESURF, (b) T-RESURF, (c) Dual-CL.

Figure 3 shows the surface potential distributions of RESURF LDMOS devices with different vertical doping profiles when the breakdown occurs. These devices have the same geometric parameters. The lines represent the analytical results of the proposed model, and the dots are the corresponding numerical results obtained by the Medici simulator. From

Table 1. Analytical expressions of different vertical doping profiles.

Vertical doping profile		Analytical expression of $N(y)$
Continuous	uniform	$N_{\rm D}$
	linear	$(N_{\rm bot}-N_{\rm sur})\,y/t_{\rm s}+N_{\rm sur}$
	Gaussian	$N_{\rm sur}\exp\left(-(y/t_{\rm s})^2\ln(N_{\rm sur}/N_{\rm bot})\right)$
Discrete	double RESURF (D-RESURF)	$\begin{cases}-P_{\rm top}, & \text{if } x\in[L_1, L_{\rm d}-L_2] \text{ and } y\in[0,t_{\rm P}]\\ N_{\rm D}, & \text{otherwise}\end{cases}$
	triple RESURF (T-RESURF)	$\begin{cases}-P_{\rm top} & ,\text{if } x\in[L_1, L_{\rm d}-L_2] \text{ and } y\in[t_{\rm N}, t_{\rm N}+t_{\rm P}]\\ N_{\rm D}, & \text{otherwise}\end{cases}$
	dual conduction layer (Dual-CL)	$\begin{cases}N_{\rm top}, & \text{if } x\in[L_1, L_{\rm d}-L_2] \text{ and } y\in[0,t_{\rm N}]\\ -P_{\rm top}, & \text{if } x\in[L_1, L_{\rm d}-L_2] \text{ and } y\in[t_{\rm N}, t_{\rm N}+t_{\rm P}]\\ N_{\rm D}, & \text{otherwise}\end{cases}$

$N_{\rm D}$: drift doping concentration; $N_{\rm sur}$, $N_{\rm bot}$: doping concentrations at the surface and at the bottom of the drift region; $P_{\rm top}$, $N_{\rm top}$: doping concentrations of the P-top layer and the N-top layer; L_1, L_2: distances of the P-top/N-top layer to the P-well/N-drift and N-drift/N^+-drain junctions; $t_{\rm N}$, $t_{\rm P}$: thicknesses of the N-top layer and the P-top layer.

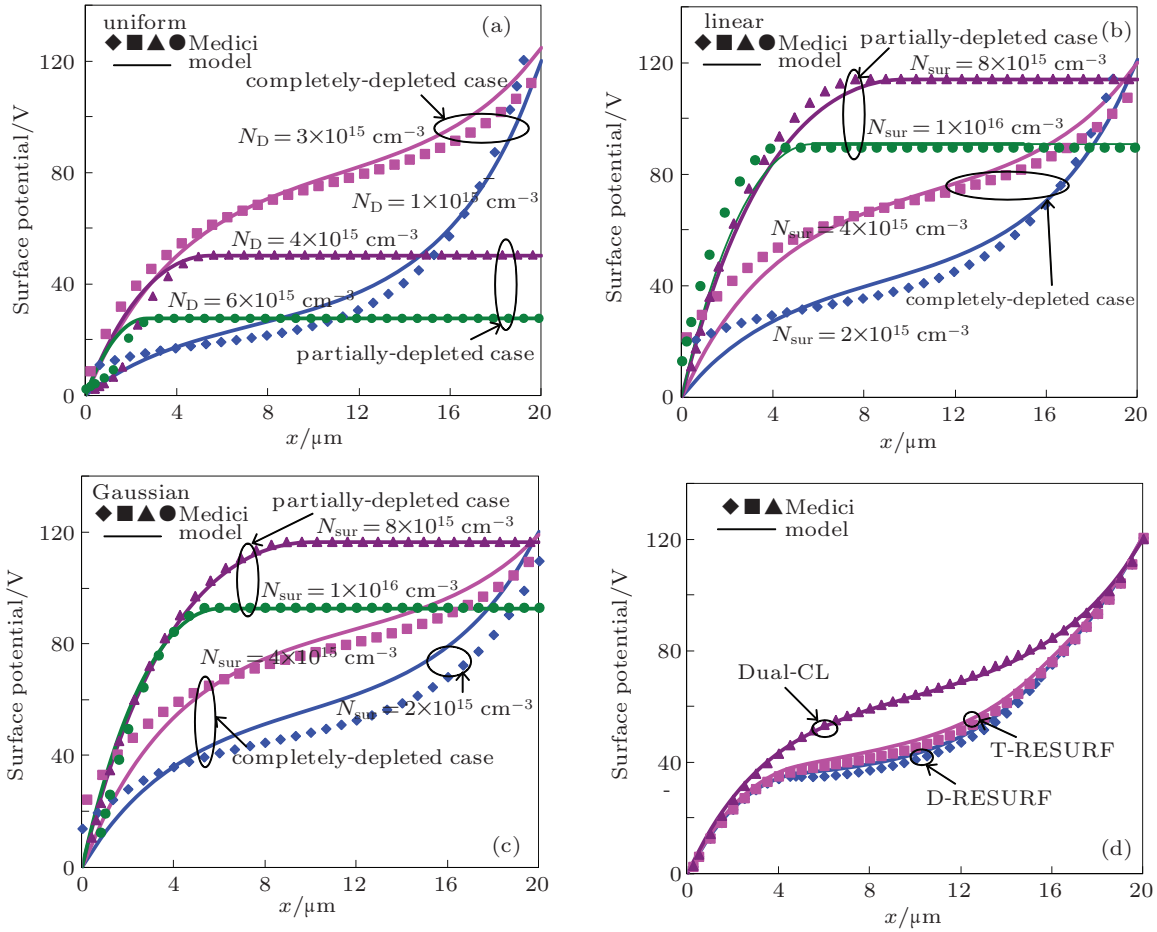


Fig. 3. (color online) The surface potential distributions of RESURF LDMOS devices with different vertical doping profiles ((a) uniform doping profile with $N(y)=N_{\rm D}$, $L_{\rm d}=20$ μm, $t_{\rm s}=5$ μm, $N_{\rm A}=1\times10^{16}$ cm^{-3}, (b) linear doping profile with $N(y)=(N_{\rm bot}-N_{\rm sur})y/t_{\rm s}+N_{\rm sur}$, $N_{\rm bot}=1\times10^{15}$ cm^{-3}, $L_{\rm d}=20$ μm, $t_{\rm s}=5$ μm, $N_{\rm A}=1\times10^{16}$ cm^{-3}, (c) Gaussian doping profile with $N(y)=N_{\rm sur}\exp[-(y/t_{\rm s})^2\ln(N_{\rm sur}/N_{\rm bot})]$, $N_{\rm bot}=1\times10^{14}$ cm^{-3}, $L_{\rm d}=20$ μm, $t_{\rm s}=5$ μm, $N_{\rm A}=1\times10^{16}$ cm^{-3}, (d) discrete doping profiles with $N_{\rm D}=3\times10^{15}$ cm^{-3}, $N_{\rm top}=6\times10^{15}$ cm^{-3}, $P_{\rm top}=1.5\times10^{15}$ cm^{-3}, $N_{\rm A}=1\times10^{16}$ cm^{-3}, $L_{\rm d}=20$ μm, $t_{\rm s}=5$ μm, $t_{\rm P}=1$ μm).

Fig. 3, one can observe that no matter whether the LDMOS devices are completely-depleted or partially-depleted and whether the vertical doping profiles are continuous or discrete, the analytical results are in a good accordance with the Medici simulation results, except for a few small discrepancies near the junctions. The discrepancies in the analytical results are due to the ignorance of the curvature and the built-in potential of junctions in the present model, and the penetration of the space charge region into the P-well and N^+-drain diffusion regions. However, these kinds of discrepancies have little effect on the breakdown characteristic analysis. The surface potentials at both boundaries of the depleted region coincide with the applied voltages, which rise from 0 V at the P-well/N-drift junction to V_d at the depletion boundary. In addition, with the increase of the drift doping concentration, the potential drop increases at the P-well/N-drift junction but reduces at the N-drift/N^+-drain junction. When the drift doping concentration is large enough, with which the depletion region cannot punch through to the N^+-drain edge, the potential drop at the N-drift/N^+-drain junction decreases to zero.

The analytical and the Medici simulation results of surface electric field distributions for RESURF LDMOS devices with different vertical doping profiles are given in Fig. 4. The results are obtained with the same conditions listed in Fig. 3. From Figs. 4(a)–4(c), it is evident that there are two electric field peaks along the silicon surface when the drift region is completely-depleted, one appears at the P-well/N-drift junction and the other at the N-drift/N^+-drain junction. The two electric field peaks strongly depend on the drift doping concentration. After being partially depleted, there is only one electric field peak at the surface of the P-well/N-drift junction, and further increasing the drift doping concentration leads to a movement of the depletion edge from the N-drift/N^+-drain junction to the P-well/N-drift junction. As shown in Fig. 4(d), the discrete doping brings a new additional electric field peak at the right end of the P-top layer. This coincides with the present and the previous numerical analysis results.[13] Therefore, we can see that the drift doping concentration is a very important parameter influencing the electric field peak, and thus determines the breakdown voltage.

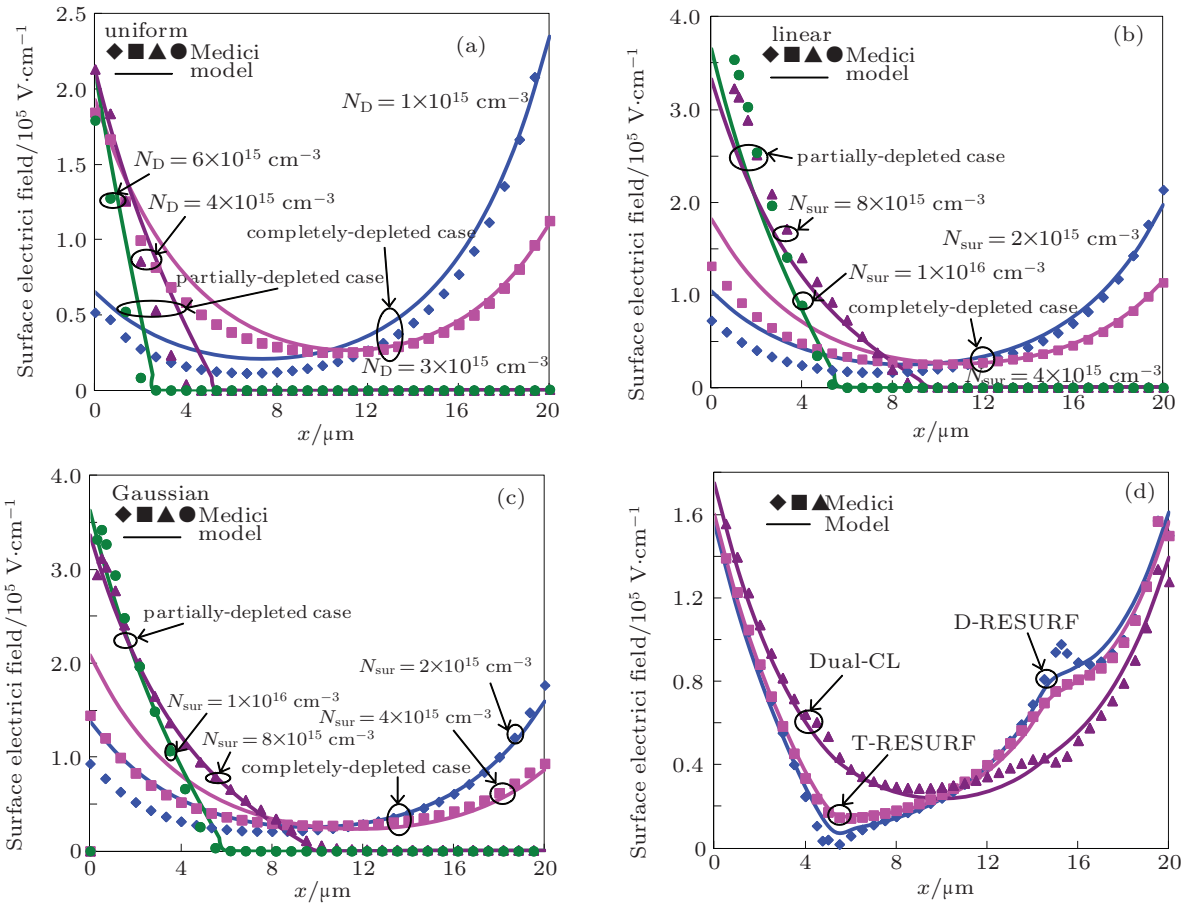


Fig. 4. (color online) Surface electric field distributions of RESURF LDMOS devices with different vertical doping profiles ((a) uniform doping profile with $N(y) = N_D$, $L_d = 20$ μm, $t_s = 5$ μm, $N_A = 1\times10^{16}$ cm^{-3}, (b) linear doping profile with $N(y) = (N_{bot} - N_{sur})y/t_s + N_{sur}$, $N_{bot} = 1\times10^{15}$ cm^{-3}, $L_d = 20$ μm, $t_s = 5$ μm, $N_A = 1\times10^{16}$ cm^{-3}, (c) Gaussian doping profile with $N(y) = N_{sur}\exp[-(y/t_s)^2\ln(N_{sur}/N_{bot})]$, $N_{bot} = 1\times10^{14}$ cm^{-3}, $L_d = 20$ μm, $t_s = 5$ μm, $N_A = 1\times10^{16}$ cm^{-3}, (d) discrete doping profiles with $N_D = 3\times10^{15}$ cm^{-3}, $N_{top} = 6\times10^{15}$ cm^{-3}, $P_{top} = 1.5\times10^{15}$ cm^{-3}, $N_A = 1\times10^{16}$ cm^{-3}, $L_d = 20$ μm, $t_s = 5$ μm, $t_P = 1$ μm).

To verify the proposed breakdown model, the results from the analytical expressions are compared with Medici numerical results. Figure 5 illustrates the analytical and numerical results of the breakdown voltage as a function of drift doping concentration for uniform-, linear-, and Gaussian-doped LDMOS devices. In order to achieve a better agreement between analytical and numerical results, the critical electric fields $E_{c,lat}$ and $E_{c,ver}$ are adjusted within the range from 2×10^5 V/cm to 5×10^5 V/cm.[22] For a given device with a light doping, the breakdown voltage increases with the increasing doping concentration due to the surface breakdown at the N-drift/N^+-drain junction, whereas, when the drift doping concentration approaches an optimal value, the highest breakdown voltage is exhibited. A further increase of the drift doping concentration will bring a rapid decrease of the breakdown voltage because of the partial depletion of the drift region. Meanwhile, the variety of the drift doping concentration can lead to a movement of the breakdown location among the N-drift/N^+-drain junction surface, the P-well/N-drift junction surface, and the interface of drift/substrate under the drain.

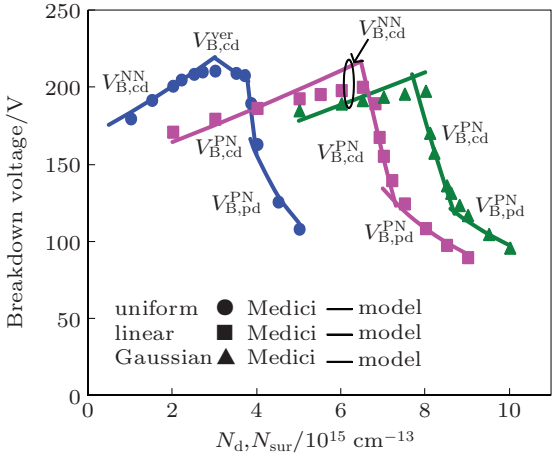


Fig. 5. (color online) Breakdown voltage as a function of doping concentration in the drift region, with $L_d = 20$ μm, $L_1 = L_2 = 5$ μm, $t_s = 5$ μm, $t_P = 1$ μm, $N_A = 2\times10^{15}$ cm^{-3}, $N_{bot} = 1\times10^{14}$ cm^{-3}, $P_{top} = 1\times10^{15}$ cm^{-3}.

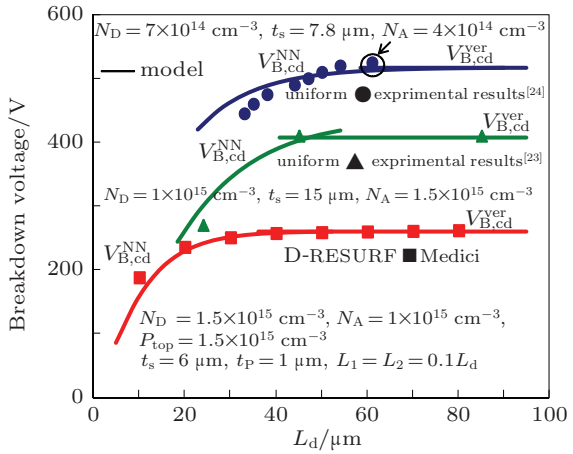


Fig. 6. (color online) Breakdown voltage as a function of the drift region length.

Figure 6 shows the calculated breakdown voltage as a function of the drift region length along with the Medici numerical results and the previous experimental results reported in Refs. [23] and [24]. Note that, the tendency of the analytical results coincides well with the experimental and numerical results. For a given set of parameters, increasing the drift region length increases the breakdown voltage up to a constant value determined by the drift/substrate junction breakdown.

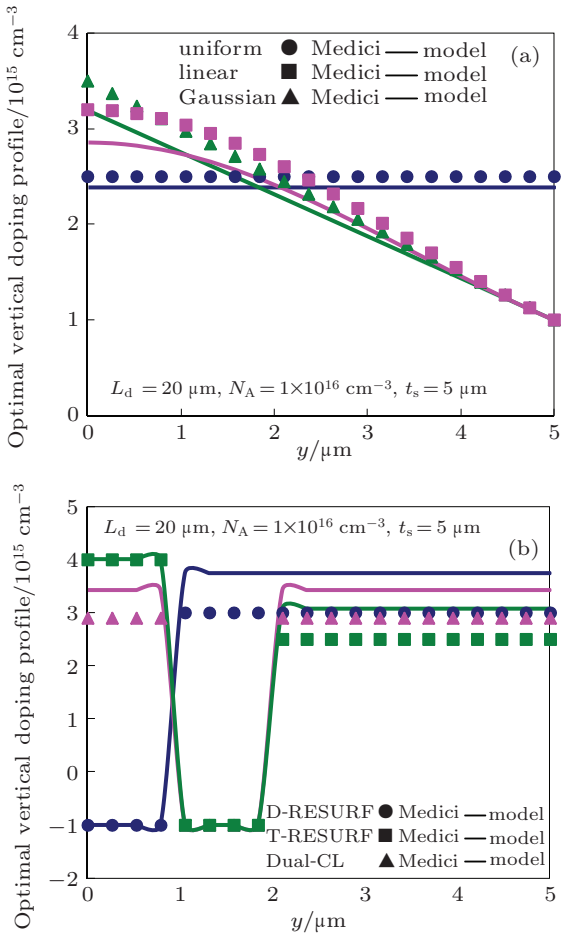


Fig. 7. (color online) The optimization of different vertical doping profiles ((a) continuous doping profiles, (b) discrete doping profiles).

In order to enhance the breakdown characteristics while maintaining the low on-resistance, obtaining an ideal surface field distribution is much needed, and the drift doping concentration is of considerable importance. Figure 7 shows the calculated analytical results and the Medici numerical results of optimal vertical doping profiles for the devices discussed above. Accordingly, the calculated analytical and numerical values of the effective concentration N_{eff} are given in Table 2. It is clear that all the values of N_{eff} are approximately equal. This is because the geometric parameters of these devices are exactly the same, then their characteristic thicknesses are almost identical, and according to Eq. (25), the effective concentrations should also be equal. In addition, according to Eq. (24), the equal effective concentration and the identical characteristic thickness lead to the same breakdown voltage.

The fact can be further confirmed by the simulated electric field distributions at breakdown in Fig. 8, the surface field distributions and the vertical field variations of the six optimized devices are consistent. Therefore, no matter whether the breakdown occurs in the lateral direction or in the vertical direction, their breakdown voltages are roughly equal. Moreover, the numerical results of breakdown voltage, the analytical results of $V_{\mathrm{B,lat.opt}}$ and $V_{\mathrm{B,cd}}^{\mathrm{ver}}$ are also listed in Table 2.

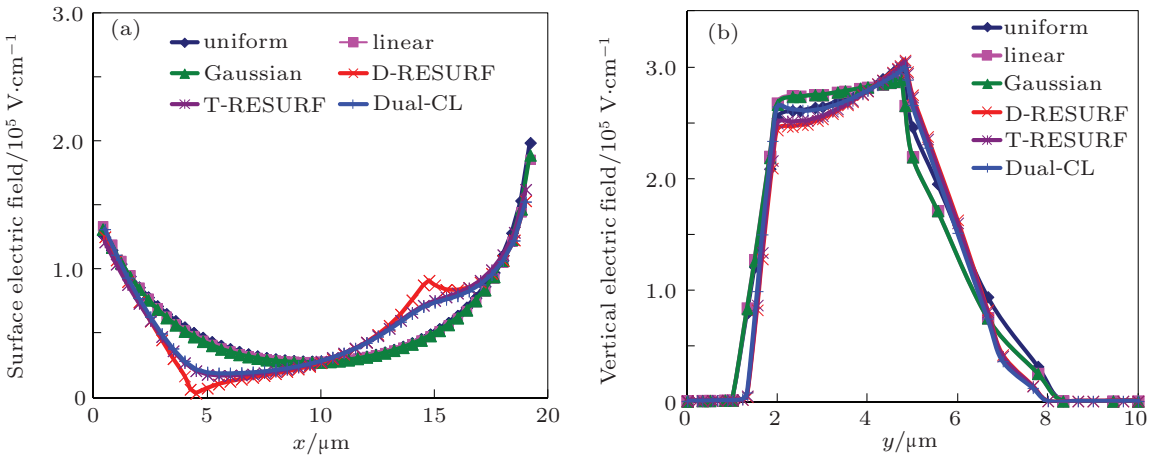


Fig. 8. (color online) Electric field distributions of the optimized LDMOS devices at breakdown: (a) surface electric field, (b) vertical electric field under drain.

Table 2. Summary of electrical performance and Baliga's FOM values of the six optimized LDMOS devices (in the on-state, $V_{\mathrm{GS}} = 5$ V, $V_{\mathrm{DS}} = 0.5$ V).

Device type	$N_{\mathrm{eff}}/10^{15}\mathrm{cm}^{-3}$ (model/Medici)	$V_{\mathrm{B,lat.opt}}$/V (model)	$V_{\mathrm{B,cd}}^{\mathrm{ver}}$/V (model)	V_{B}/V (Medici)	$R_{\mathrm{on}}/\Omega\mathrm{cm}$ (Medici)	FOM/W·cm^{-1} (Medici)
Uniform	2.39/2.50	120.4	123.6	125.4	13.1	1200
Linear	2.39/2.56	122.9	126.1	120.7	11.9	1220
Gaussian	2.38/2.62	125.3	125.3	120.4	12.1	1200
D-RESURF	2.20/2.35	126.2	122.2	120.8	13.4	1092
T-RESURF	2.26/2.47	125.5	124.5	120.6	14.3	1020
Dual-CL	2.30/2.63	129.6	129.8	121.2	15.3	959

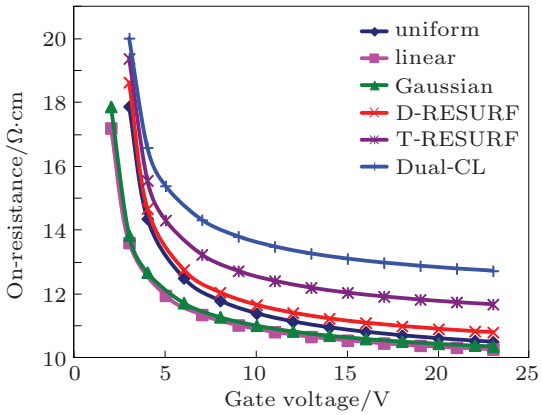


Fig. 9. (color online) Dependencies of the gate voltage on the on-resistance for the optimized LDMOS devices.

Figure 9 gives the influence of the gate voltage on the on-resistance for the optimized devices. The drain voltage is 0.5 V in simulation. It must be noticed that although the optimization of the vertical doping profile has little influence on the maximization of the breakdown voltage, it has some effects on the on-resistance. The linear-doped device shows the lowest on-resistance. The Dual-CL device is the worst case. Table 2 summarizes the overall comparison among the six optimized LDMOS devices. It seems that the vertical linear doping profile is the best choice for obtaining the lowest on-resistance R_{on} and the highest Baliga's FOM ($V_{\mathrm{B}}^2/R_{\mathrm{on}}$) value.

6. Conclusion

This paper focuses on general analytical models of bulk silicon lateral power devices with arbitrary vertical doping profiles in the drift region. Firstly, by discretizing the drift doping profile vertically and solving the 2D Poisson's equation, an effective concentration of the drift region is introduced, and analytical expressions for the surface potential and electric field distributions are further presented. Secondly, the breakdown voltages for both the completely-depleted and the partially-depleted cases are obtained based on the electric field peaks and the concept of critical electric field. Thirdly, a generalized RESURF criterion that is available for various drift doping profiles is derived. According to the proposed models, the surface potential and electric field distributions of the drift regions with the uniform, linear, Gaussian, and some dis-

crete doping profiles are investigated in detail. The dependencies of the breakdown voltage on the drift doping concentration and the drift region length are discussed respectively. The mentioned vertical doping profiles are also optimized to maximize the breakdown voltage while maintaining the low on-resistance. Finally, it is proved that the maximum breakdown voltage is independent of the drift doping profile, and just relies on the geometric parameters of the device. When the geometric parameters of the device are set, the optimal effective concentration of the drift region and the maximum breakdown voltage are equal to those of the optimal uniform-doped device. All the analytical results are verified by the numerical results and the previous experimental results. Thus, the analytical models proposed here afford an effective way to reveal the influence of the vertical doping profile on the RESURF effect and provide a theoretical basis for optimizing the drift vertical doping profile.

References

[1] Apples J, Vaes H and Verhoeven J 1979 *Proc. IEDM* p. 238
[2] Erlbacher T, Bauer A and Frey L 2010 *IEEE Electron Dev. Lett.* **31** 464
[3] Ludikhuize A 2000 *Proc. ISPSD* p. 11
[4] Vestling L, Olsson J and Eklund K 2002 *Solid-State Electron.* **46** 1177
[5] Chung S and Han S 1998 *IEEE Trans. Electron. Dev.* **45** 1374
[6] He J and Zhang X 2001 *Microelectronics Journal* **32** 655
[7] Li Q, Zhang B and Li Z J 2007 *Research and Progress of SSE* **27** 540 (in Chinese)
[8] Li Q, Zhang B and Li Z J 2008 *Acta Phys. Sin.* **57** 1891 (in Chinese)
[9] Hu X R, Zhang B, Luo X R, Wang Y G, Lei T F and Li Z J 2012 *Chin. Phys. B* **21** 78502
[10] Sun W F and Shi L X 2004 *Solid-State Electron.* **48** 799
[11] Meng J, Gao S and Chen J N 2005 *Journal of Semiconductors* **26** 1383 (in Chinese)
[12] Wu J, Fang J, Zhang B and Li Z J 2004 *Proc. ICSICT* p. 349
[13] Luo X R, Yao G L, Zhang Z Y, Jiang Y H, Zhou K, Wang P, Wang Y G, Lei T F, Zhang Y X and Wei J 2012 *Chin. Phys. B* **21** 68501
[14] Hua T T, Guo Y F and Sheu G 2010 *Proc. ICSICT* p. 1850
[15] Disney D, Paul A, Darwish M, Basecki R and Rumennik V 2001 *Proc. ISPSD* p. 399
[16] Sheu G, Yang S M, Chang Y F and Tsaur S C 2010 *Jpn. J. Appl. Phys.* **49** 074301
[17] Sheu G, Lin Y H, Tseng W C, Yang S M, Chen C N and Guo Y F 2010 *ECS Transactions on Design and Device Engineering* **27** 103
[18] Lu S L, Sun Z L, Sun W F and Shi L X 2005 *Chinese Journal of Semiconductors* **26** 2286
[19] Han S, Kim H and Chung S 2000 *Microelectronics Journal* **31** 685
[20] Li Q, Zhu J L, Wang W D and Wei X M 2011 *Chin. Phys. B* **20** 117202
[21] Qiao M, Zhuang X, Wu L J, Zhang W T, Wen H J, Zhang B and Li Z J 2012 *Chin. Phys. B* **21** 108502
[22] Hu S D, Zhang B and Li Z J 2009 *Chin. Phys. B* **18** 315
[23] Colak S 1981 *IEEE Trans. Electron. Dev.* **28** 1455
[24] Wildi E, Gray P, Chow T, Chang H and Cornell M 1982 *IEDM Tech. Dig.* p. 268